Geophysical Research Letters

Key Points:
- Nitrate and oxygen were measured with sensors on profiling floats for time periods up to 5 years
- Nitrate is removed by denitrification or anammox in the Bay of Bengal at the lowest oxygen concentrations
- The amount of nitrate loss in the Bay of Bengal is limited by events that raise oxygen levels

Supporting Information:
- Supporting Information S1

Correspondence to:
K. S. Johnson,
johnson@mbari.org

Oxygen Variability Controls Denitrification in the Bay of Bengal Oxygen Minimum Zone

Kenneth S. Johnson[1] (iD)**, Stephen C. Riser[2]** (iD)**, and M. Ravichandran[3]** (iD)

[1]Monterey Bay Aquarium Research Institute, Moss Landing, CA, USA, [2]School of Oceanography, University of Washington, Seattle, WA, USA, [3]National Centre for Polar and Ocean Research, Vasco da Gama, Goa, India

Abstract Nitrate limits productivity in much of the ocean. Nitrate residence time is a few thousand years, and changes in nitrate loss could influence ocean productivity. Major sinks for nitrate are denitrification and anaerobic ammonia oxidation in the oxygen minimum zones (OMZs). The Bay of Bengal OMZ is anomalous because large amounts of nitrate loss do not occur there, while nitrate is removed in the nearby OMZ of the Arabian Sea. Observations of nitrate and oxygen made over 5 years by 20 profiling floats equipped with chemical sensors in the Bay of Bengal and the Arabian Sea are used to understand why nitrate is removed rapidly in the Arabian Sea but not in the Bay of Bengal. Our results confirm that nitrate is poised for removal in the Bay of Bengal. However, highly variable oxygen concentrations inhibit its loss. Nitrate loss is regulated by physical oceanographic processes that introduce oxygen.

Plain Language Summary Denitrification is a microbial process that removes nitrate, a compound essential for phytoplankton production, from seawater. Denitrification occurs in the absence of oxygen. Most denitrification in the oceanic water column occurs in three oxygen minimum zones, the Eastern Tropical North Pacific, the Eastern Tropical South Pacific, and the Arabian Sea. The Bay of Bengal is a fourth oxygen minimum zone, but little nitrate loss occurs there. Our profiling float observations show that the Bay of Bengal is poised for denitrification to occur, as found in prior studies. However, we find that frequent events raise oxygen concentrations above levels where denitrification occurs. The amount of denitrification, relative to the Arabian Sea, is set by fraction of time that oxygen is elevated. Onset of large-scale denitrification would require a shift in the ocean physics that transport the water with elevated oxygen concentration.

1. Introduction

Denitrification (both classical heterotrophic denitrification and anaerobic ammonium oxidation) in the oxygen minimum zones (OMZs) of the world ocean is a major control on the mean concentration of ocean nitrate (e.g., Codispoti et al., 2001; Gruber, 2008; Gruber & Sarmiento, 1997). Water column denitrification is concentrated in three primary locations: the OMZs of the Eastern Tropical North Pacific, the Eastern Tropical South Pacific, and the Arabian Sea (AS; DeVries et al., 2012). The role of a fourth major OMZ, the Bay of Bengal (BoB), has remained enigmatic. Biogeochemical estimates of dentrification in the BoB show little evidence for large amounts of denitrification (Bristow et al., 2016; Howell et al., 1997; Naqvi et al., 1996).

The fixed nitrogen residence time in the ocean is ~1,500 to 3,000 years (Codispoti et al., 2001; Gruber, 2008), and any large changes in nitrate loss rates will lead to variability in nitrate concentration (Codispoti et al., 2001; Deutsch et al., 2011). Understanding the processes that control nitrate loss in the BoB is therefore a critical step for prediction of future ocean productivity. Modeling studies, which compare the dynamics of the OMZ in the BoB with that of the AS, suggest the lack of denitrification in the BoB results from lower productivity and carbon export on its western boundary (McCreary et al., 2013) or slower remineralization of organic carbon, as expressed by the vertical scale length over which carbon is consumed (Al Azhar et al., 2017). Bristow et al. (2016) demonstrate that a community of denitrifiers is present in the BoB. They suggest that denitrification by this community was inhibited by a trace of dissolved oxygen that was observed. Sarma and Bhaskar (2018) used a 3-year-long oxygen record from a profiling float to reexamine the oxygen levels in the BoB and processes that control them. They found higher mean oxygen levels than seen by Bristow et al. (2016), which were generated by periodic anticyclonic eddies passing through the BoB. However, the

profiling float examined by Sarma and Bhaskar (2018) was located further south than the region sampled by Bristow et al. (2016).

Here we examine the multiyear records of nitrate and oxygen concentration reported by profiling floats in the BoB and the AS to contrast the processes that regulate denitrification in these systems. The data records span more than 5 years, which ensures an adequate representation of variability in these systems. These records provide a much more complete view of system variability than the results obtained from short-term research studies. We find that denitrification does remove nitrate in the BoB when oxygen is depleted. However, external processes regularly inject substantial (~5 to 10 μmol/kg) amounts of oxygen into this OMZ. This observation is consistent with the findings of Sarma and Bhaskar (2018). The high oxygen in these events inhibits denitrification. As a result, denitrification in the BoB appears to be controlled by an oxygen source term driven by ocean physics.

2. Materials and Methods

We deployed one profiling float with nitrate and oxygen sensors in each of the AS and the BoB. These floats were Teledyne Webb Research Apex floats assembled and tested at the University of Washington (Riser et al., 2018). Nitrate sensors were In Situ Ultraviolet Spectrophotometer (ISUS) sensors built and calibrated at the Monterey Bay Aquarium Research Institute (Johnson et al., 2013; Johnson & Coletti, 2002). All nitrate data were processed according to BGC-Argo protocols (Johnson et al., 2018). The computation of nitrate concentration does not explicitly consider nitrite, which also has a weak absorption spectrum (Johnson & Coletti, 2002). If nitrite is present, the computed nitrate concentration is approximately (NO_3^-) + 0.5 (NO_2^-). However, there was no evidence, in the form of systematic changes in absorption spectrum residuals, to indicate the presence of nitrite concentrations above the amount detectable in the presence of nitrate (~10% of the background nitrate concentration). The apparent absence of nitrite may reflect temporal variability as nitrite has been detected in this region (Naqvi, 1994).

Oxygen was measured with Aanderaa optode sensors (Bittig et al., 2018; Körtzinger et al., 2005). Oxygen concentration was computed following BGC-Argo protocols (Thierry et al., 2016). In addition to the two floats with nitrate sensors, the oxygen concentrations reported by 18 floats with oxygen sensors, which were deployed by Argo India, were utilized. These floats were a mix of NKE Provor III and Teledyne Webb Research Apex floats that were equipped with Aanderaa optode oxygen sensors. Quality control procedures for the sensors are described previously (Johnson et al., 2017).

The floats profiled to the surface at 5- to 10-day intervals, making measurements as they rose. Between profiles, the floats parked at 1,000-m depth, except float 5903712 in the BoB. Its ballasting did not allow it to reach depths below 800 m. The other floats reported measurements beginning between 1,000 and 2,000 m. The nitrate vertical sampling resolution varied between floats but was generally 5 m in the upper 100 and 10 m to near 400 m and 20 m below that.

3. Data

All profiling float data were downloaded from the Argo Global Data Assembly Centers. A list of the floats utilized in this study is provided in Table S1 in the supporting information. Shipboard measurements in the AS and BoB were obtained from the GLODAPv2 database (Olsen et al., 2016), which was downloaded in Ocean Data View format (Schlitzer, 2018). Recent ship measurements in the BoB on the I09N line (cruise 33RR20160321) were downloaded from the CLIVAR and Carbon Hydrographic Data Office (https://cchdo.ucsd.edu). Recent ship measurements in the AS were obtained from the Geotraces Intermediate Data Product (http://www.geotraces.org).

4. Results

The time/depth sections of oxygen and nitrate concentration observed by floats 5903586 (AS) and 5903712 (BoB) are shown in Figure 1. Maps of the float trajectories are shown in Figure S1 in the supporting information. Float 5903586 was deployed in the core of the high nitrite region of the AS, where denitrification is most rapid (Naqvi, 1994). The float was rapidly advected to the western margin of the AS, where oxygen
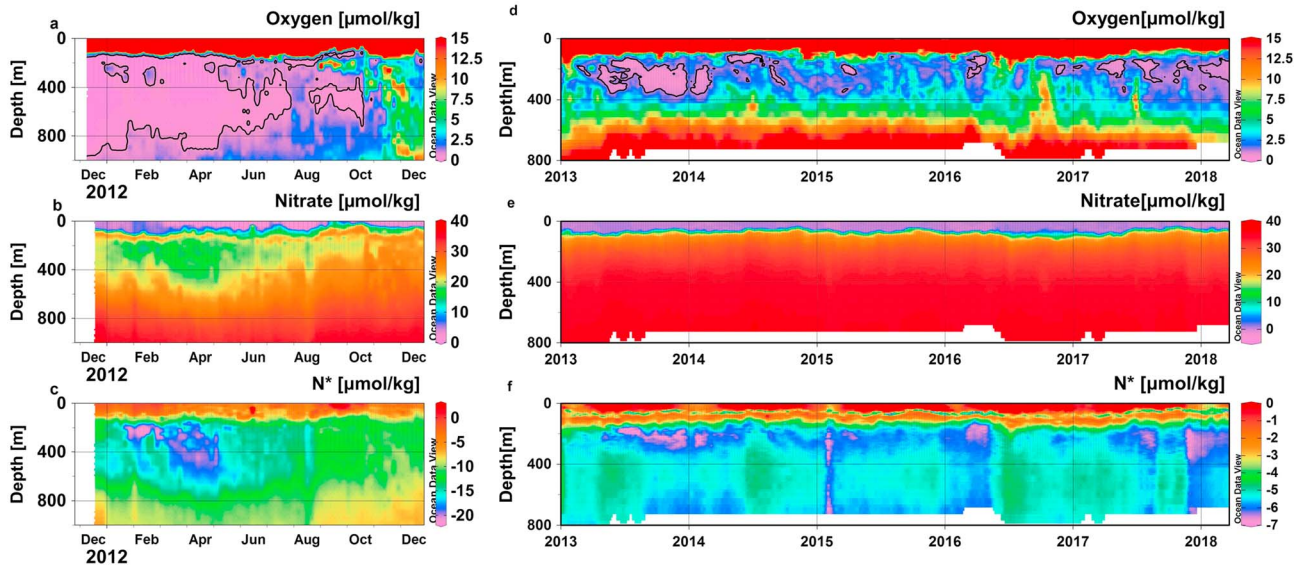
Figure 1. Observed oxygen and nitrate concentrations and computed N* values by (a–c) float 5903586 in the Arabian Sea and (d–f) float 5903712 in the Bay of Bengal. Data for float 5903586 are limited to the time period when it was east of 58°E. Ocean Data View (Schlitzer, 2018) was used to prepare the sections.

concentrations increased. No data are shown after that time (profile 60, 18 October 2012). Float 5903712 remained in the northern BoB for 5 years.

Large depletions of nitrate are apparent in the AS record from January through July of 2012, while the float remained in low oxygen waters. These depletions are apparent as a reversal in the general increase of nitrate concentration with depth, which occurs within the OMZ (Figure 2). Loss of nitrate can be quantified by several methods. Here we compute the variable N* (Gruber & Sarmiento, 1997) to assess nitrate removal

$$N^* = \left((\mathrm{NO_3^-}) - 16 \times \left(\mathrm{PO_4^{3-}}\right) + 2.9\right) \tag{1}$$

N* is a tracer that reflects the balance between nitrate and phosphate at Redfield proportions. The constant 2.9 sets the mean ocean value of N* near zero, and large, negative N* values indicate removal of nitrate, relative to the amount expected from the phosphate. Some recent applications of N* omit the constant 2.9 (e.g., Deutsch et al., 2011). We have retained the constant here as it sets surface values of N* close to zero in both the BoB and AS. The value of this constant offset in N* has no impact on the conclusions discussed below.

Profiling floats do not measure phosphate concentration. The concentration of phosphate corresponding to each nitrate measurement was therefore determined using a multiple linear regression (MLR) equation

$$\left(\mathrm{PO_4^{3-}}\right)_{\mathrm{AS}} = 1.075 + 0.00756 \times \mathrm{AOU} - 0.0325 \times t \tag{2}$$

$$\left(\mathrm{PO_4^{3-}}\right)_{\mathrm{BoB}} = 1.808 + 0.00521 \times \mathrm{AOU} - 0.0552 \times t \tag{3}$$

Equations (2) and (3) were fitted with data from the GLODAPv2 data set (Olsen et al., 2016) in the depth range from 100 to 1,200 m in the AS or the BoB (Figure S2). AOU is apparent oxygen utilization (oxygen solubility-measured oxygen, μmol/kg), and t is the temperature (°C). The use of MLR equations to predict biogeochemical properties in the ocean interior is well established (Carter et al., 2018; Juranek et al., 2011; Williams et al., 2016). Additional parameters beyond AOU and temperature that were considered in the equations (salinity, density, and depth) resulted in large increases in the variance inflation factor (Juranek et al., 2011) and they were not included.

Conceptually, the constant and linear temperature terms in equations (2) and (3) account for changes in preformed phosphate concentration with water mass properties. The AOU term accounts for phosphate produced by oxidation of organic matter using oxygen. The equations neglect any contribution to the phosphate pool due to remineralization of organic matter by suboxic processes. However, the ratio of
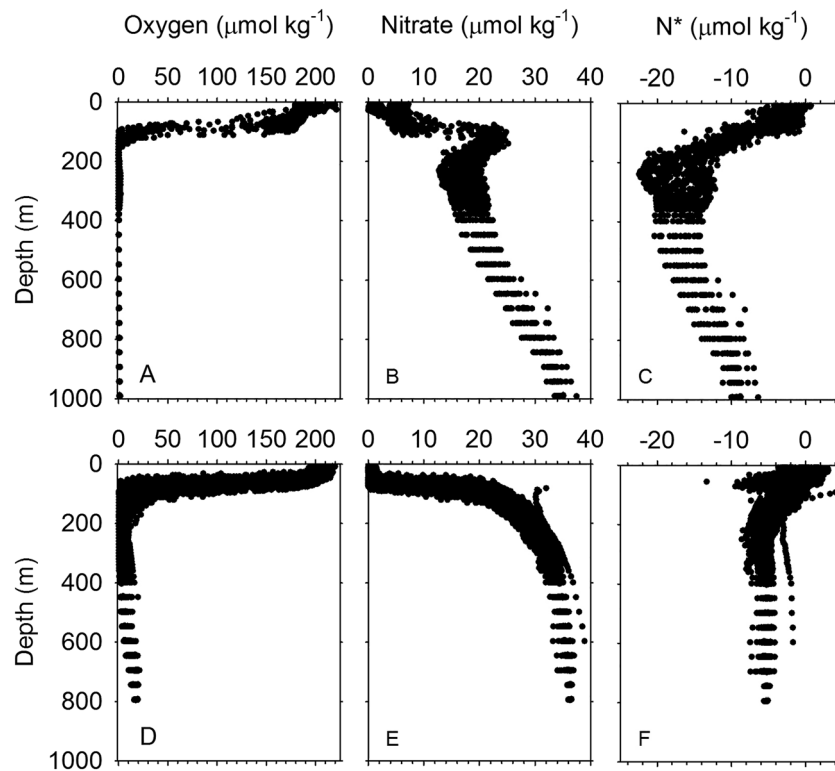
Figure 2. Vertical profiles of oxygen, nitrate, and *N** from (a–c) float 5903586 in the Arabian Sea and (d–f) float 5903712 in the Bay of Bengal. Data for 5903586 span the time from 17 December 2011 to 24 April 2012 (profiles 1 to 26) when the float was in the core the OMZ (Figure 1). All profiles are shown for 5903712.

nitrate reduced to carbon oxidized during denitrification is near one (104 N:106 C; Gruber, 2008). If 10 μmol/kg of nitrate were removed by oxidizing organic material with Redfield C:P ratios (106:1), then the biases due to neglect of suboxic processes in equations (2) and (3) would be order of 0.1 μmol/kg phosphate (10 × 1/106) at most. This would lead to uncertainty in *N** by about 1.6 μmol/kg in the regions of largest nitrate loss. The MLR equations reproduce phosphate concentration with a standard error of the regression of 0.08 μmol/kg (AS) and 0.06 μmol/kg (BoB). More than 94% of the residuals around each equation fall within 0.15 μmol/kg of the MLR predictions (Figure S2). This confirms that there are not large anomalies in phosphate within the OMZs that are created by suboxic reactions. Recent shipboard data from the OMZs of the BoB and AS, which were not included in GLODAPv2, were used as an independent data set to validate the phosphate predictions (Figure S2). Thus, we are confident that equations (2) and (3) can be used to estimate *N** values to within about 1.5 μmol/kg, which is equivalent to a 10% uncertainty at large nitrate depletions.

The *N** profiles in the AS reach values as low as −22 μmol/kg, indicating loss of large amounts of nitrate (Figure 2c). Relative to *N** values above and below the oxygen minimum (or at the same depth in the BoB), the AS has lost a mean of 10 μmol/kg nitrate within the depth range from 150 to 400 m. This is comparable to a variety of estimates of nitrate removal in the AS using N_2 gas measurements (Chang et al., 2012; Devol et al., 2006; DeVries et al., 2012) and anomalies in nitrate profiles (Howell et al., 1997; Morrison et al., 1999; Naqvi, 1994). In contrast, the BoB float does not show a similar reversal in nitrate concentration (Figure 2e). The *N** profiles in the BoB show only a weak depletion in the core of the oxygen minimum, relative to values found above and below. This is consistent with prior work (Bristow et al., 2016; Howell et al., 1997).

The oxygen concentrations measured by the float array at depths from 220 to 260 m, where *N** reaches a minimum, are shown in Figure 3. Oxygen optode sensors have some uncertainty in absolute calibration near zero oxygen, but they are exceptionally precise and quite stable (Bittig et al., 2018). Sensors exposed to anoxic conditions will generate stable signals with little or no variation in the output. This is seen for
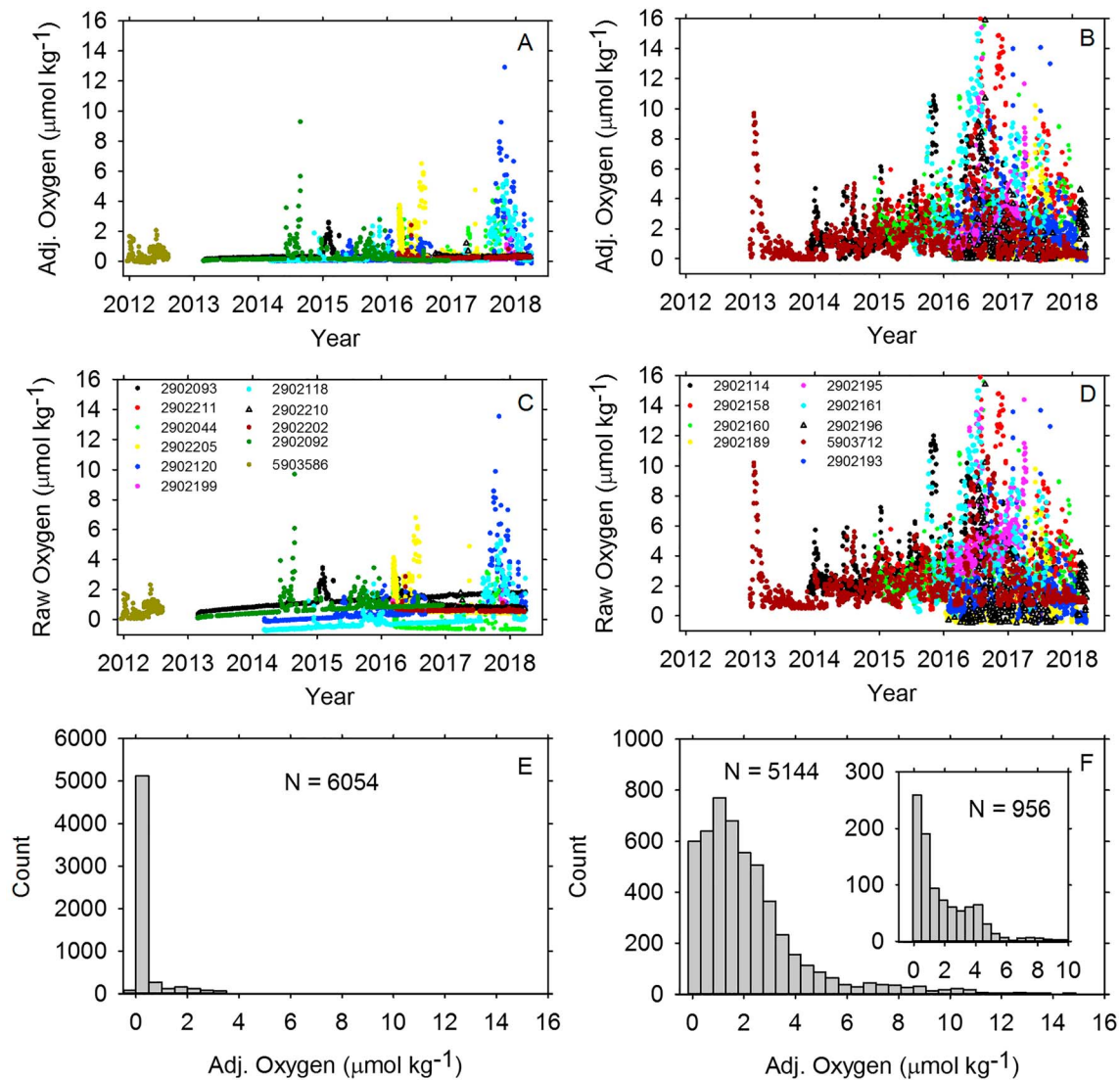
Figure 3. Adjusted oxygen measurements in the (a) Arabian Sea east of 60°W and in the (b) Bay of Bengal (BoB). Adjustment parameters for sensor calibration offset and drift are listed in supporting information Table S1. (c and d) Raw sensor measurements are shown. (e and f) Histograms of the adjusted oxygen concentrations in the AS and BoB are shown. The inset in (f) shows the histogram of BoB oxygen values north of 15°N and west of 90°E. All measurements were in the depth range from 220 to 260 m at the core of the N^* minima. Data points are colored by WMO number of the floats. Data for float 5903586 are limited to the time period when it was east of 60°E.

the raw oxygen data from the array of 11 floats in the AS (Figure 3c). The records of AS oxygen concentration in the core of the N^* minimum show almost no variability relative to the smallest oxygen amounts that affect optode sensor response (order of 0.05 μmol/kg), other than slow, linear drifts in sensor output. There are only occasional oxygen excursions away from these linear trends. The long runs of oxygen concentration with root mean square variability <0.1 μmol/kg about linear trends must correspond to periods with oxygen levels less than 0.1 μmol/kg. The oxygen sensor data were adjusted to correct for calibration offsets and slow drift by removing the offsets and a linear trend from the data for each sensor. The correction methods are detailed in Text S1 in the supporting information and Figure S3. The method is similar to that used by Wojtasiewicz et al. (2018). The absolute values of sensor drifts were <0.5 μmol · kg^{-1} · year^{-1}, and offsets were <1 μmol/kg (Table S1). The adjusted oxygen values are shown in Figures 3a and 3b for all floats.

About 85% of the adjusted AS oxygen data in the 220- to 260-m depth range are below a value of 0.5 μmol/kg (Figure 3e), which is a conservative detection limit for corrected sensor data (Text S1). In contrast, only 16%
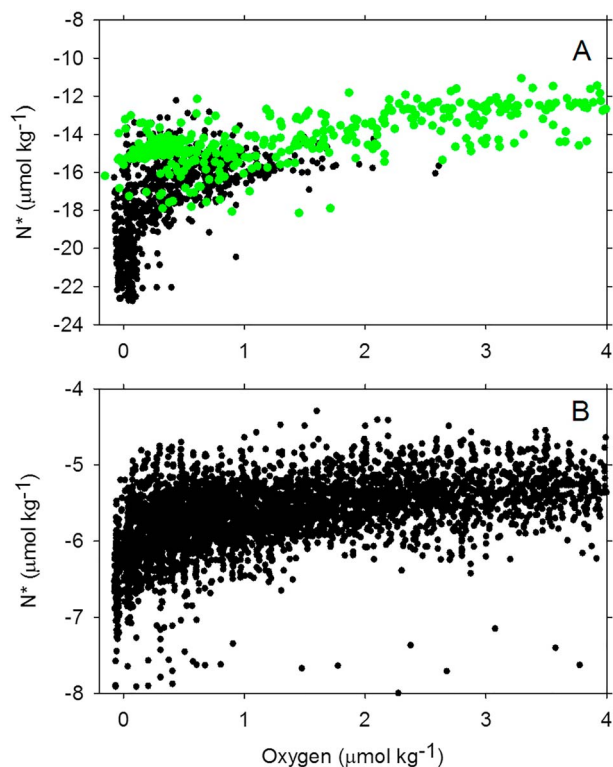
Figure 4. N^* values versus the adjusted oxygen concentrations in the (a) Arabian Sea and (b) Bay of Bengal. In the Arabian Sea, the black symbols are samples east of 60°E in the core of the OMZ, while the green samples are west of 60°E. Samples were from the depth range 200 to 400 m.

of the BoB data lie below this level (Figure 3f). Long runs of stable oxygen concentrations less than 0.5 μmol/kg were seldom seen for any of the oxygen sensors on the nine floats in the BoB (Figure 3b). These concentrations are well above the 0.05 μmol/kg levels below which oxygen must decrease for full turn on of denitrification (Dalsgaard et al., 2014; Thamdrup et al., 2012).

Events with oxygen concentrations greater than 5 μmol/kg were observed 9% of the time by the floats in the BoB, while these were much rarer (0.4% of observations) in the OMZ of the AS. No large difference in these observations results if data are selected on density surfaces, rather than depth. A more detailed assessment of nitrate loss in both basins was made by plotting N^* versus the adjusted oxygen concentration in the depth range between 200 and 400 m (Figure 4). The N^* data were binned by 0.1 μmol/kg increments in adjusted oxygen. The BoB float (Figure 4b) shows a modest drop in N^* at the lowest oxygen concentration bin (−0.05 to 0.05 μmol/kg). The N^* value in the lowest bin was significantly lower (Student's t-test, $p < 0.01$, $N = 179$) than the N^* value in the 0.05 to 0.15 μmol/kg bin ($N = 215$) and at any higher oxygen levels. The mean decrease in N^* in this lowest bin, relative to N^* values at an oxygen of 3 to 4 μmol/kg, was 1.1 μmol/kg. This was consistent with prior geochemical estimates of denitrification (Bristow et al., 2016).

In contrast, the AS float shows an average 6.5 μmol/kg decrease in N^* at the lowest oxygen bin, relative to values at 3 to 4 μmol/kg O_2 (Figure 4a). These higher oxygen values were only found west of 60°E. The N^* value of this lowest oxygen bin (−0.05 to 0.05 μmol/kg) was again significantly lower ($p < 0.01$, $N = 792$) than the value in the next bin (0.05 to 0.15 μmol/kg, $N = 135$) or any subsequent oxygen bins.

The ratio of the observed N^* depletion in the AS to BoB, relative to the values near 3 μmol/kg O_2 in each basin, was 6.5/1.1 = 5.9. This value was similar to the fraction of samples where the observed oxygen was less than 0.5 μmol/kg in each basin (85%/14% = 6.1). It is very likely that the fraction of samples with oxygen less than 0.5 μmol/kg in each basin is similar to the fraction of time that most locations in the core of each OMZ have similarly low oxygen, given the large number of float profiles and multiple years of data in each basin,. This would not be true only if there were some unknown bias that led floats to preferentially sample low oxygen water. This suggests that the amount of denitrification is proportional to the time that oxygen concentrations are less than sensor detection limits. These conclusions are supported by the estimates of denitrification in the BoB and AS by Bristow et al. (2016). They found that biogenic N_2 production in the AS exceeded that in the BoB by a factor of 8.3. We conclude that the potential for denitrification in the BoB is similar to that of the AS, but the amount of nitrate converted to N_2 is limited by more frequent elevated oxygen levels in the BoB.

Horizontal spatial gradients in oxygen distributions are present in the BoB, and the fractions of time that oxygen is less than 0.5 μmol/kg will not be the same everywhere. For example, the histogram of oxygen distributions in the NW corner of the BoB (north of 15°N and west of 90°E) is shown as an inset in Figure 3f. This is the region sampled by Bristow et al. (2016). The oxygen histogram in the NW corner is skewed to lower concentrations than for the BoB as a whole. As a result, oxygen was less than 0.5 μmol/kg in 26% of the float data in the NW corner. The water sampled by Bristow et al. may represent a similar period of time when low oxygen was present. However, the overall distribution of data implies that these periods of very low oxygen (<0.5 μmol/kg) are not the most common condition.

The long-term observations with profiling floats show that denitrification in the BoB is inhibited by a process that is quite different than the mechanisms previously suggested (Al Azhar et al., 2017; Bristow et al., 2016; McCreary et al., 2013). We find highly variable oxygen concentrations that are frequently above the 0.2 μmol/kg level observed to inhibit denitrification rates by 50% or the 0.9 μmol/kg level that causes a similar reduction in anammox rates (Dalsgaard et al., 2014). Thamdrup et al. (2012) suggest even lower oxygen

concentrations limit denitrification, based on observations showing nitrite accumulation only when oxygen is less than 0.05 μmol/kg. Our observations of frequent concentrations above the critical levels for denitrification contrast with the conclusion that oxygen is poised at low levels in the nmol/kg concentration range (Bristow et al., 2016). McCreary et al. (2013) and Al Azhar et al. (2017) find that enhanced remineralization of organic carbon in the AS, which is driven by various mechanisms, leads to the lower oxygen and greater denitrification than in the BoB. However, McCreary et al. (2013) also note that there is strong seasonality in carbon export but little seasonality in OMZ oxygen concentrations of the BoB. They conclude that remineralization rates in the OMZ are not sufficient to deplete oxygen in 1 year. The profiling float oxygen data also show no seasonality in the BoB OMZ (data not shown), despite the large, short-term temporal variability shown in Figure 3. If loss rates are relatively low, the variability requires frequent inputs of oxygen bearing water to the OMZ of the BoB that sustain a higher and more variable oxygen environment as compared to the AS (Sarma & Bhaskar, 2018; Figure 3). Denitrification only begins when the oxygen transported by these episodic events is depleted. This is a subtle, but important distinction relative to a mechanism where small variability in a removal term may deplete oxygen. Oxygen must be depleted from the high values found in these events before denitrification can begin.

The episodic, high oxygen events in the BoB are likely driven by mesoscale eddies. Previous modeling (Lachkar et al., 2016; Resplandy et al., 2012) and observational (Kumar et al., 2004; Sardessai et al., 2007; Sarma et al., 2016; Sarma & Bhaskar, 2018) studies all point to the importance of eddies in controlling oxygen levels in these environments. For example, the depth of the oxycline in both the AS and BoB is strongly related to sea surface height variations driven by mesoscale eddies (Prakash et al., 2013). Glider observations in the northwest AS demonstrate the role of eddies in transporting oxygen (Queste et al., 2018). There is little seasonal variability in the frequency of eddies found in the BoB, but there are large, interannual changes in the eddy number (Chen et al., 2012).

5. Conclusions

The BoB is poised for denitrification to occur. Prior studies suggested that small, biological forcing mechanisms, such as a change in carbon flux, would force the BoB into a state where denitrification was frequent (Al Azhar et al., 2017; Bristow et al., 2016). The BoB appears much more resistant to such change, as oxygen concentrations are often well above levels where denitrification has been reported (Bristow et al., 2016; Dalsgaard et al., 2014) to commence. This variability in oxygen concentration leads to much less denitrification than seen in the AS. Small changes in the mean oxygen concentration would not greatly change the amount of time oxygen is near zero when the system is dominated by episodic events. Prior work suggests that these events are associated with mesoscale eddies. Onset of large-scale denitrification in the BoB would likely require a large shift in mesoscale eddy distributions. The large, interannual variations in eddy number that were reported by Chen et al. (2012) may influence the oxygen state and denitrification. It is possible that a significant reduction in eddy transport of oxygen into the OMZ would result in the onset of large scale denitrification in the BoB.

References

Al Azhar, M., Lachkar, Z., Lévy, M., & Smith, S. (2017). Oxygen minimum zone contrasts between the Arabian Sea and the Bay of Bengal implied by differences in remineralization depth. *Geophysical Research Letters*, *44*, 11,106–11,114. https://doi.org/10.1002/2017GL075157

Bittig, H. C., Körtzinger, A., Neill, C., van Ooijen, E., Plant, J. N., Hahn, J., et al. (2018). Oxygen optode sensors: Principle, characterization, calibration, and application in the ocean. *Frontiers in Marine Science*, *4*, 429. https://doi.org/10.3389/fmars.2017.00429

Bristow, L. A., Callbeck, C. M., Larsen, M., Altabet, M. A., Dekaezmacker, J., Forth, M., et al. (2016). N$_2$ production rates limited by nitrite availability in the Bay of Bengal oxygen minimum zone. *Nature Geoscience*, *10*(1), 24–29. https://doi.org/10.1038/NGEO2847

Carter, B. R., Feely, R. A., Williams, N. L., Dickson, A. G., Fong, M. B., & Takeshita, Y. (2018). Updated methods for global locally interpolated estimation of alkalininity, pH, and nitrate. *Limnology and Oceanography: Methods*, *16*, 119–131.

Chang, B. X., Devol, A. H., & Emerson, S. R. (2012). Fixed nitrogen loss from the eastern tropical North Pacific and Arabian Sea oxygen deficient zones determined from measurements of N$_2$:Ar. *Global Biogeochemical Cycles*, *26*, GB3030. https://doi.org/10.1029/2011GB004207

Chen, G., Wang, D., & Hou, Y. (2012). The features and interannual variability mechanism of mesoscale eddies in the Bay of Bengal. *Continental Shelf Research*, *47*, 178–185. https://doi.org/10.1016/j.csr.2012.07.011

Codispoti, L. A., Brandes, J. A., Christensen, J. P., Devol, A. H., Naqvi, S. W. A., Paerl, H. W., & Yoshinari, T. (2001). The oceanic fixed nitrogen and nitrous oxide budgets: Moving targets as we enter the Anthropocene? *Scientia Marina*, *65*(Suppl. 2), 85–105. https://doi.org/10.3989/scimar.2001.65s285

Dalsgaard, T., Stewart, F. J., Thamdrup, B., De Brabandere, L., Revsbech, N. P., Ulloa, O., et al. (2014). Oxygen at nanomolar levels reversibly suppresses process rates and gene expression in anammox and denitrification in the oxygen minimum zone off northern Chile. *MBio*, *5*(6), e01966–e01914. https://doi.org/10.1128/mBio.01966-14

Deutsch, C., Brix, H., Ito, T., Frenzel, H., & Thompson, L. (2011). Climate-forced variability of ocean hypoxia. *Science*, *333*(6040), 336–339. https://doi.org/10.1126/science.1202422

Devol, A. H., Uhlenhopp, A. G., Naqvi, S. W. A., Brandes, J. A., Jayakumar, D. A., Naik, H., et al. (2006). Denitrification rates and excess nitrogen gas concentrations in the Arabian Sea oxygen deficient zone. *Deep-Sea Research, Part I*, *53*(9), 1533–1547. https://doi.org/10.1016/j.dsr.2006.07.005

DeVries, T., Deutsch, C., Primeau, F., Chang, B. X., & Devol, A. (2012). Global rates of water-column denitrification derived from nitrogen gas measurements. *Nature Geoscience*, *5*(8), 547–550. https://doi.org/10.1038/ngeo1515

Gruber, N. (2008). The marine nitrogen cycle: overview and challenges. In D. G. Capone, D. A. Bronk, M. R. Mulholland, & E. J. Carpenter (Eds.), *Nitrogen in the marine environment* (pp. 1–50). Burlington, MA: Academic Press.

Gruber, N., & Sarmiento, J. L. (1997). Global patterns of marine nitrogen fixation and denitrification. *Global Biogeochemical Cycles*, *11*(2), 235–266. https://doi.org/10.1029/97GB00077

Howell, E. A., Doney, S. C., Fine, R. A., & Olson, D. B. (1997). Geochemical estimates of denitrification in the Arabian Sea and the Bay of Bengal during WOCE. *Geophysical Research Letters*, *24*(21), 2549–2552. https://doi.org/10.1029/97GL01538

Johnson, K. S., & Coletti, L. J. (2002). In situ ultraviolet spectrophotometry for high resolution and long term monitoring of nitrate, bromide and bisulfide in the ocean. *Deep Sea Research, Part I*, *49*(7), 1291–1305. https://doi.org/10.1016/S0967-0637(02)00020-1

Johnson, K. S., Coletti, L. J., Jannasch, H. W., Sakamoto, C. M., Swift, D., & Riser, S. C. (2013). Long-term nitrate measurements in the ocean using the In Situ Ultraviolet Spectrophotometer: Sensor integration into the Apex profiling float. *Journal of Atmospheric and Oceanic Technology*, *30*(8), 1854–1866. https://doi.org/10.1175/JTECH-D-12-00221.1

Johnson, K. S., Pasqueron de Fommervault, O., Serra, R., D'Ortenzio, F., Schmechtig, C., Claustre, H., & Poteau, A. (2018). Processing Bio-Argo nitrate concentration at the DAC level. doi:10.13155/46121

Johnson, K. S., Plant, J. N., Coletti, L. J., Jannasch, H. W., Sakamoto, C. M., Riser, S. C., et al. (2017). Biogeochemical sensor performance in the SOCCOM profiling float array. *Journal of Geophysical Research: Oceans*, *122*, 6416–6436. https://doi.org/10.1002/2017JC012838

Juranek, L. W., Feely, R. A., Gilbert, D., Freeland, H., & Miller, L. A. (2011). Real-time estimation of pH and aragonite saturation state from Argo profiling floats: Prospects for an autonomous carbon observing strategy. *Geophysical Research Letters*, *38*, L17603. https://doi.org/10.1029/2011GL0.48580

Körtzinger, A., Schimanski, J., & Send, U. (2005). High quality oxygen measurements from profiling floats: A promising new technique. *Journal of Atmospheric and Oceanic Technology*, *22*(3), 302–308. https://doi.org/10.1175/JTECH1701.1

Kumar, S. P., Nuncio, M., Narvekar, J., & Kumar, A. (2004). Are eddies nature's trigger to enhance biological productivity in the Bay of Bengal? *Geophysical Research Letters*, *31*, L07309. https://doi.org/10.1029/2003GL019274

Lachkar, Z., Smith, S., Lévy, M., & Pauluis, O. (2016). Eddies reduce denitrification and compress habitats in the Arabian Sea. *Geophysical Research Letters*, *43*, 9148–9156. https://doi.org/10.1002/2016GL069876

McCreary, J. P. Jr., Yu, Z., Hood, R. R., Vinaychandran, P. N., Furue, R., Ishida, A., & Richards, K. J. (2013). Dynamics of the Indian-Ocean oxygen minimum zones. *Progress in Oceanography*, *112*, 15–37.

Morrison, J. M., Codispoti, L. A., Smith, S. L., Wishner, K., Flagg, C., Gardner, W. D., et al. (1999). The oxygen minimum zone in the Arabian Sea during 1995. *Deep-Sea Research, Part II*, *46*(8-9), 1903–1931. https://doi.org/10.1016/S0967-0645(99)00048-X

Naqvi, S. W. A. (1994). Denitrification processes in the Arabian Sea. *Proceedings of the Indiana Academy of Sciences*, *103*, 279–300.

Naqvi, S. W. A., Shailaja, M. S., Kumar, M. D., & Sen Gupta, R. (1996). Respiration rates in subsurface waters of the northern Indian Ocean: Evidence for low decomposition rates of organic matter within the water column in the Bay of Bengal. *Deep-Sea Research, Part II*, *3*, 73–81.

Olsen, A., Key, R. M., van Heuven, S., Lauvset, S. K., Velo, A., Lin, X., et al. (2016). The Global Ocean Data Analysis Project version 2 (GLODAPv2)—An internally consistent data product for the world ocean. *Earth System Science Data*, *8*(2), 297–323. https://doi.org/10.5194/essd-8-297-2016

Prakash, S., Prakash, P., & Ravichandran, M. (2013). Can oxycline depth be estimated using sea level anomaly (SLA) in the northern Indian Ocean? *Remote Sensing Letters*, *4*(11), 1097–1106. https://doi.org/10.1080/2150704X.2013.842284

Queste, B. Y., Vic, C., Heywood, K. J., & Piontkovski, S. A. (2018). Physical controls on oxygen distribution and denitrification potential in the north west Arabian Sea. *Geophysical Research Letters*, *45*, 4143–4152. https://doi.org/10.1029/2017GL076666

Resplandy, L., Lévy, M., Bopp, L., Echevin, V., Pous, S., Sarma, V. V. S. S., & Kumar, D. (2012). Controlling factors of the oxygen balance in the Arabian Sea's OMZ. *Biogeosciences*, *9*(12), 5095–5109. https://doi.org/10.5194/bg-9-5095-2012

Riser, S. C., Swift, D., & Drucker, R. (2018). Profiling floats in SOCCOM: Technical capabilities for studying the Southern Ocean. *Journal of Geophysical Research: Oceans*, *123*, 4055–4073. https://doi.org/10.1002/2017JC013419

Sardessai, S., Ramaiah, N., Kumar, S. P., & de Sousa, S. N. (2007). Influence of environmental forcings on the seasonality of dissolved oxygen and nutrients in the Bay of Bengal. *Journal of Marine Research*, *65*(2), 301–316. https://doi.org/10.1357/002224007780882578

Sarma, V. V. S. S., & Bhaskar, T. V. S. (2018). Ventilation of oxygen to oxygen minimum zone due to anticyclonic eddies in the Bay of Bengal. *Journal of Geophysical Research: Biogeosciences*, *123*, 2145–2153. https://doi.org/10.1029/2018JG004447

Sarma, V. V. S. S., Rao, G. D., Viswanadham, R., Sherin, C. K., Salisbury, J., Omand, M. M., et al. (2016). Effects of freshwater stratification on nutrients, dissolved oxygen, and phytoplankton in the Bay of Bengal. *Oceanography*, *29*(2), 222–231. https://doi.org/10.5670/oceanog.2016.54

Schlitzer, R. (2018). Ocean data view. Retrieved from http://odv.awi.de.

Thamdrup, B., Dalsgaard, T., & Revsbech, N. P. (2012). Widespread functional anoxia in the oxygen minimum zone of the eastern South Pacific. *Deep Sea Research, Part I*, *65*, 36–45. https://doi.org/10.1016/j.dsr.2012.03.001

Thierry, V., Bittig, H., Gilbert, D., Kobayashi, T., Kanako, S., & Schmid, C. (2016). Processing Argo oxygen data at the DAC level. https://doi.org/10.13155/39795

Williams, N. L., Juranek, L. W., Johnson, K. S., Feely, R. A., Riser, S. C., Talley, L. D., et al. (2016). Empirical algorithms to estimate water column pH in the Southern Ocean. *Geophysical Research Letters*, *43*, 3415–3422. https://doi.org/10.1002/2016GL068539

Wojtasiewicz, B., Trull, T. W., Udaya Bhaskar, T. V. S., Gauns, M., Prakash, S., Ravichandran, M., et al. (2018). Autonomous profiling float observations reveal the dynamics of deep biomass distributions in the denitrifying oxygen minimum zone of the Arabian Sea. *Journal of Marine Systems*. https://doi.org/10.1016/j.jmarsys.2018.07.002